

# Field Application of the Combined Membrane-Interface Probe and Hydraulic Profiling Tool (MiHpt)

by Wesley McCall, Thomas M. Christy, Daniel Pipp, Mads Terkelsen, Anders Christensen, Klaus Weber, and Peter Engelsen

---

## Abstract

The Membrane-Interface Probe and Hydraulic Profiling Tool (MiHpt) is a direct push probe that includes both the membrane interface probe (MIP) and hydraulic profiling tool (HPT) sensors. These direct push logging tools were previously operated as separate logging systems for subsurface investigation in unconsolidated formations. By combining these two probes into one logging system the field operator obtains useful data about the distribution of both volatile organic contaminants (VOCs) and relative formation permeability in a single boring. MiHpt logging was conducted at a chlorinated VOC contaminated site in Skuldelev, Denmark, to evaluate performance of the system. Formation cores and discrete interval slug tests are used to assess use of the HPT and electrical conductivity (EC) logs for lithologic and hydrostratigraphic interpretation. Results of soil and groundwater sample analyses are compared to the adjacent MiHpt halogen specific detector (XSD) logs to evaluate performance of the system to define contaminant distribution and relative concentrations for the observed VOCs. Groundwater profile results at moderate to highly contaminated locations were found to correlate well with the MiHpt-XSD detector responses. In general, soil sample results corresponded with detector responses. However, the analyses of saturated coarse-grained soils at the site proved to be unreliable as demonstrated by high RPDs for duplicate samples. The authors believe that this is due to pore water drainage observed from these cores during sampling. Additionally, a cross section of HPT pressure and MiHpt-XSD detector logs provides insight into local hydrostratigraphy and formation control on contaminant migration.

---

## Introduction

Determining the spatial distribution of volatile organic contaminants (VOCs) in heterogeneous unconsolidated formations is a difficult challenge. The growing consensus in the industry is that high-resolution contaminant distribution data is one of the critical factors needed to develop a conceptual site model and a requirement for the design of effective remediation systems (EPA 2010, 2011, 2013; ITRC 2010, 2011). An associated factor is the hydrostratigraphic architecture of the formation being investigated. Through many years of field experience in the industry and research we have learned that small-scale changes in hydraulic conductivity is a very important factor controlling the distribution, migration, and ultimately the remediation of VOCs and other contaminants in the subsurface (Sanchez-Vila 1996; Wilson et al. 1997; EPA 1998; Bright et al. 2002; Schulmeister et al. 2003; Zheng and Gorelick 2003; Bowling et al. 2005; Payne et al. 2008; Kober et al. 2009; Bohling et al. 2012; Devlin et al. 2012).

Direct push (DP) logging of soils and unconsolidated formations formally began with cone penetration testing

(CPT) for geotechnical site characterization in the 1930s (Lunne et al. 1997). Over the last 25 years DP technology has provided several new tools and methods for sampling and logging that have helped improve geo-environmental site characterization quality and resolution (Christy and Spradlin 1992; McCall et al. 2006). A percussion driven electrical conductivity (EC) logging probe and system was introduced in 1994 (Christy et al. 1994). This probe is primarily used for inferring lithology based on the bulk EC of the unconsolidated material penetrated (Schulmeister et al. 2003, 2004; Wilson et al. 2005), but it also provides qualitative information on permeability. The membrane interface probe (MIP) was introduced in 1996 as a tool for the investigation of the distribution of VOCs (Christy 1996). The MIP system has been widely used to investigate releases of petroleum hydrocarbons (e.g., gasoline) and chlorinated VOCs such as trichloroethylene (TCE) and perchloroethylene (PCE) (Costanza and Davis 2000; Griffin and Watson 2002; McAndrews et al. 2003; McCall et al. 2006; Ravella et al. 2007; Considine and Robbat 2008; Bronders et al. 2009; Kurup 2009; Bumberger et al. 2011). The MIP probe has a semi-permeable membrane that is heated to approximately 100 °C. The membrane allows VOCs to diffuse from the formation into a carrier gas stream flowing behind the membrane. The carrier gas is transported through a trunk line to gas phase detectors mounted in a

gas chromatograph (GC) at the surface. The detectors provide total VOC detection without analyte specificity. The detectors most commonly used with the MIP system are the photo-ionization detector (PID), flame ionization detector (FID), halogen specific detector (XSD), and electron capture detector (ECD). The MIP probe also includes an EC array to help with definition of formation lithology. The MIP probe is usually advanced in 30-cm increments with approximately 1-min resident time at each depth interval to allow volatiles in the formation to diffuse across the membrane and flow up the transfer line to the GC. The MIP system provides logs of total VOC contamination at the selected advancement increment and bulk formation EC at the centimeter scale.

The hydraulic profiling tool (HPT) was later developed to provide logs of relative formation permeability (Geoprobe 2006a, 2007; Kober et al. 2009), and estimates of hydraulic conductivity (McCall and Christy 2010; McCall 2010, 2011) at centimeter-scale resolution. The HPT system provides information about changes in formation permeability by measuring the pressure required to inject small volumes of water into unconsolidated formations (Geoprobe 2006a, 2007). Water is injected at a flow rate of about 300 mL/min into the formation through a small screen mounted on the side of the probe as the tool is advanced at the rate of 2 cm/s. A down-hole transducer measures the pressure required to inject water into the formation as the probe is advanced while an up-hole flow meter monitors the flow rate. The HPT probe includes an EC array to simultaneously provide measurements of bulk formation EC. The HPT system provides logs of pressure, flow, and EC in real time as the tool is advanced.

Until recently MIP logs for VOC contamination and HPT logs to assess formation permeability were obtained with separate probes in two separate logging runs. In the years 2011 to 2012 Geoprobe® combined the MIP and HPT probes into a single Membrane-Interface Probe and Hydraulic Profiling Tool (MiHpt) probe (Figure 1) that is also equipped with an EC dipole array. The MiHpt system simultaneously provides logs of total VOC contamination for up to four GC detectors, HPT pressure and flow rate, as well as bulk formation EC. The logs are viewed real-time on a computer screen as the probe is advanced and the data are stored.

The purpose of this work was to field test the MiHpt system in Skuldelev, Denmark. This site is underlain by glacial to late glacial deposits consisting of silts and clays to sand and gravel with sporadic cobbles and boulders underlain by glacial till. The site is contaminated with PCE, TCE, and their degradation products (NIRAS A/S 2010, 2012). Soil and groundwater were sampled at selected log locations and depths and submitted for laboratory analysis. Results of the sample analyses are compared to the adjacent MiHpt XSD detector logs to evaluate performance of the system to define contaminant distribution and relative concentrations. The HPT pressure, EC, and estimated hydraulic conductivity logs are compared to soil cores and slug tests at selected locations to evaluate the performance of the system to assess lithology and relative permeability.



**Figure 1.** The MiHpt probe body is 520 mm (20.5 inches) long and about 45 mm (1.75 inches) in diameter. The heater block at the MIP membrane is heated to 100 °C to enhance VOC diffusion from the formation across the membrane.

## Equipment and Methods

### MiHpt System

The MiHpt system is a combination of the membrane interface probe (MIP) and HPT as described above. Appropriate operating procedures and guidance were followed at all times as the MiHpt logs were obtained for this study (Geoprobe 2007, 2009; ASTM 2007a). The primary up-hole components of the system used in this study are shown in Figure S1. The Model MP6507 MIP Controller (Geoprobe Systems, Salina, Kansas) regulates gas flow to and the temperature of the MiHpt probe. The MIP controller also has inputs for up to four gas phase detectors (Geoprobe 2004); three were used with the system in Skuldelev. These included a PID, an FID, and an XSD that were operated from an SRI Model 310c GC (SRI Instruments, Torrance, California). The K6303 Series HPT Flow Module (Geoprobe Systems, Salina, Kansas) contains a metering pump that provided flow via trunk line to the HPT injection port at 0 to 500 mL/min. Flow rate was controlled by the metering pump and digitally monitored for the log. Both the HPT and MIP controllers were connected to the FI6003 Data Acquisition System (Geoprobe Systems, Salina, Kansas) for operation in the field. This field instrument received input from the controllers and the probe and provided digital output to a laptop computer. The Direct Image (DI) Acquisition® software (Geoprobe Systems, Salina, Kansas) displayed the MIP detector response, HPT pressure and flow as well as the EC log onscreen vs. depth, as the probe was advanced. The data were saved to file for later review and reporting.

Prior to each log, quality assurance (QA) tests were performed on the MiHpt probe and system according to manufacturer and ASTM specifications (Geoprobe 2007, 2009; ASTM 2007a). The QA tests were performed to verify the system was providing appropriate detector responses for contaminant concentration, accurate HPT pressure, and EC measurements. Data from all of the QA tests were saved in an information file that was stored with the respective MiHpt log file.

The MiHpt probe was advanced with a probe machine using both static push and percussion hammer, as needed. The MiHpt probe was typically advanced at 2 cm/s over 30-cm increments and then stopped for about 45 s to allow for contaminant diffusion across the membrane and for the MIP carrier gas to flow from the probe to the GC detectors at the surface (carrier gas trip time). At desired depths probe advancement was stopped, the HPT water flow was turned off and a pressure dissipation test was performed to determine the local piezometric pressure. Dissipation tests were run for each log at selected depths of interest below the water table. After each log was completed the HPT pressure and HPT flow rate were used to calculate a log of estimated hydraulic conductivity (*Est. K*) using the DI Viewer® software. The *Est. K* calculation is based on a simple empirical model (McCall and Christy 2010; McCall 2010, 2011),

$$Est. K = 21.14 \times \ln \left( \frac{Q}{P_c} \right) - 41.71, \quad (1)$$

where  $Q$  is the HPT flow rate and  $P_c$  the corrected HPT pressure at each depth increment.

### Soil and Groundwater Sampling and Analysis

Before samples were collected at a location, replicate MiHpt logs were conducted to verify that contaminant concentrations did not vary significantly in the area to be studied (Figure S2a). The depth intervals for sampling soil and groundwater were

selected not only based on detector responses, but also on the HPT pressure and the EC log. Soil cores generally were taken continuously across the zone of indicated contamination, often extending above and below the zone where feasible to assess the range of detector responses observed with the MiHpt detectors. Soil cores were collected with the DT325 dual tube system (Figure S2b) (ASTM 2007b; Geoprobe 2011a; NIRAS 2012; McCall 2012). En Core® tools (En Novative Technologies, Inc.) were used to collect 25-g sub samples. The sub samples were immediately transferred to sample vials (Figure S2c) and transported daily to the laboratory for analysis. After VOC subsampling was completed the PVC sample liners were cut longitudinally for lithologic logging.

MIP detector responses, HPT pressure, and EC responses were examined to select screen intervals for groundwater sampling. SP16 groundwater sampling tools (Geoprobe 2006b; ASTM 2007c) were installed at the selected locations and screens were set over the desired intervals. The screen intervals were typically 30 cm long to provide discrete interval groundwater samples for VOCs. Once the screens were set they were surged and purged with a simple check valve (Geoprobe PN GW4210) for development. After purging 10 to 20 L for development a model MB470 mechanical bladder pump (McCall 2005; Geoprobe 2011b) was installed to perform purging and water quality monitoring (Figure S2d), followed by low flow sampling (ASTM 2007d). Water quality parameters (temperature, pH, specific conductance, dissolved oxygen [DO], oxidation reduction potential [ORP]) were monitored in a closed flow cell until parameters stabilized. Periodically, turbidity was monitored with an Oakton model T100 turbidity meter. At most locations turbidity was below 20 NTU before groundwater sampling for VOCs was conducted. Once water quality had stabilized groundwater was collected directly into 40-mL volatile organic analysis (VOA) vials.

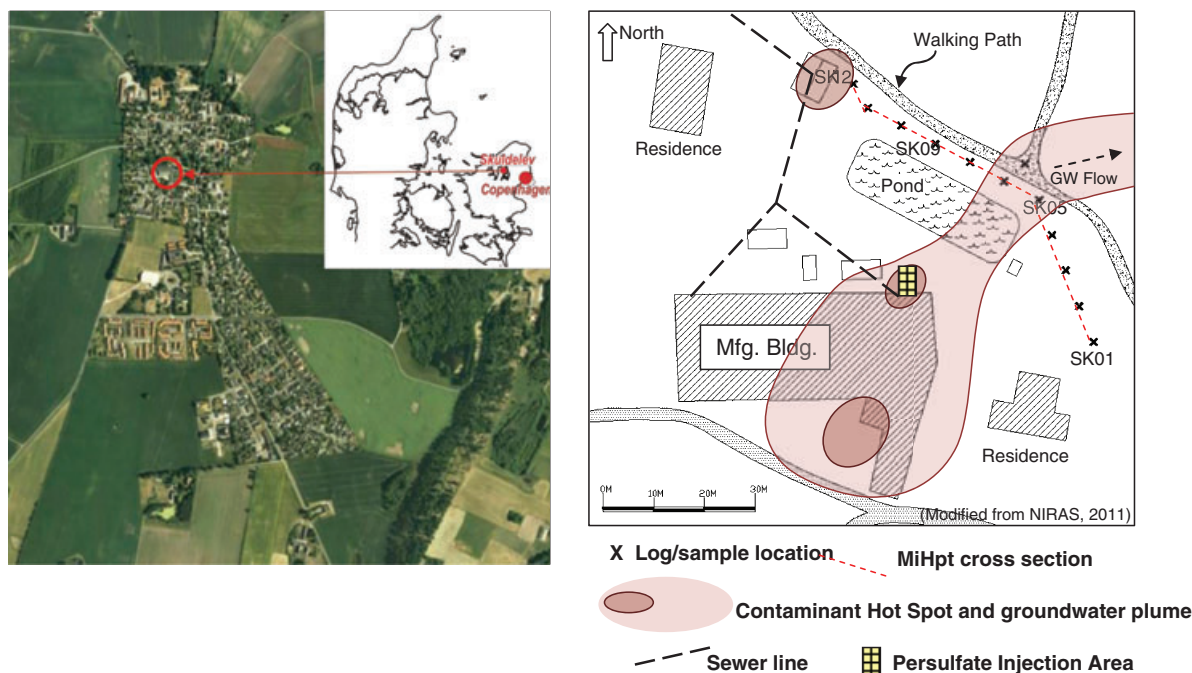


Figure 2. Site location map for Skuldelev, Denmark, and site map with log-sample locations.



All laboratory analyses for chlorinated VOCs were performed using gas chromatography-mass spectrometry. All sample holding times were met and all laboratory QA protocols were achieved as defined by method SW846 5035A for soils and method SW846 8260B for water samples (<http://www.epa.gov/osw/hazard/testmethods/sw846/online/>). All samples were analyzed at the *Milana A/S* laboratory ([www.milana.dk](http://www.milana.dk)).

## Results and Discussion

Field work was conducted at Skuldelev in coordination with NIRAS A/S and the Environmental Department of the Capital Region of Denmark during October, 2011 (McCall

2012; NIRAS 2012). After review of existing site information (NIRAS A/S 2010) the field team set up and ran a transect of MiHpt logs across the site (Figure 2). Analyses of soil (Table S1) and groundwater (Table S2) samples from the site identified PCE, TCE, cis-1, 2-dichloroethene (c-DCE), trans-1, 2-dichloroethene (t-DCE), and vinyl chloride (VC) as the primary contaminants. The following sections discuss log and sample results at the site and assess performance of the MiHpt system relative to the sample results.

### Lithology and Permeability

The HPT pressure log along with injection flow rate and EC are used to assess lithology and relative formation permeability from MiHpt logs (Figure 3). The total pressure

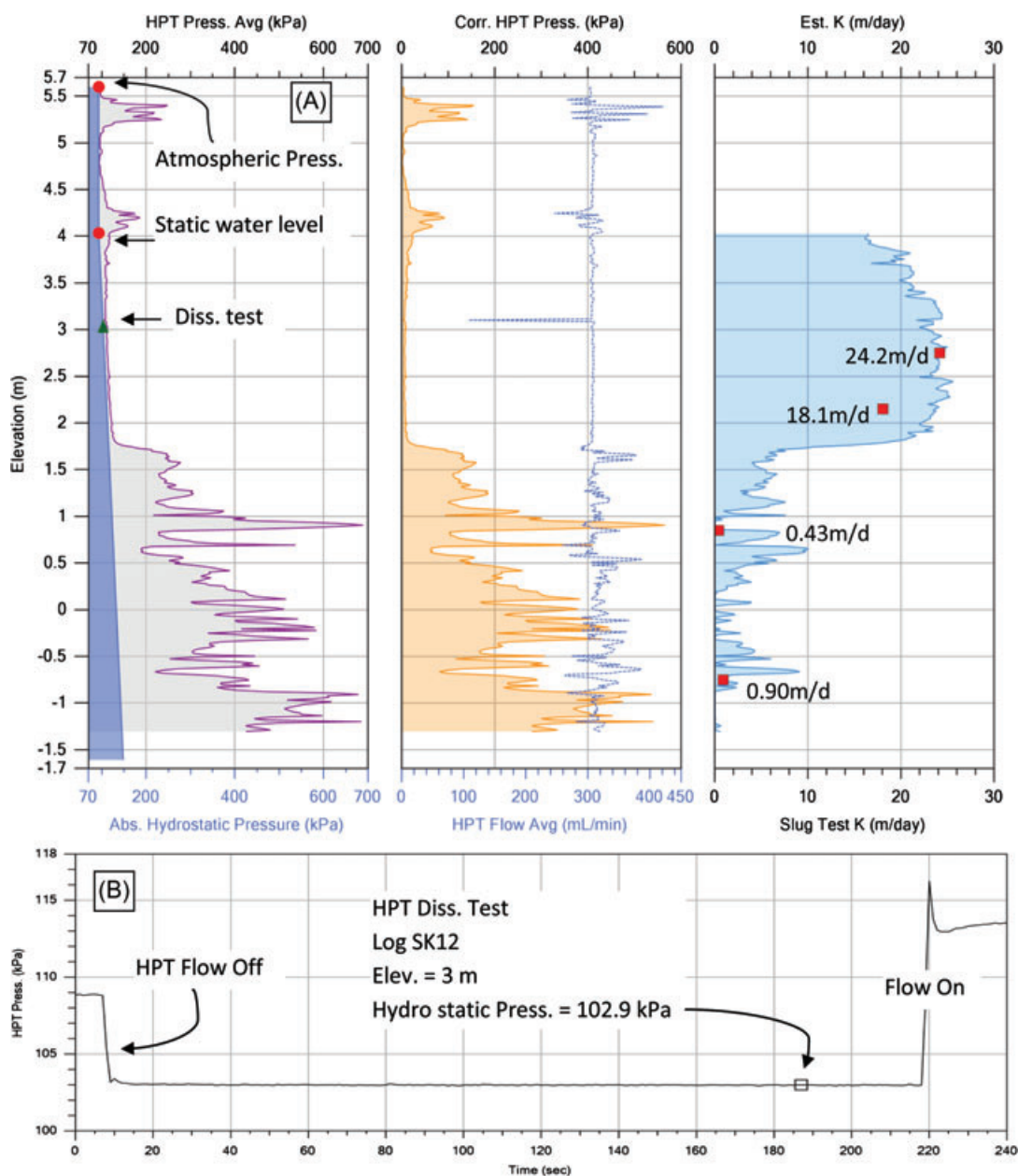


Figure 3. The SK12 log (A) displaying parameters used to correct the raw HPT pressure and calculate the estimated hydraulic conductivity (Est. K) log. Dissipation test (B) conducted at elevation of 3 m to establish local hydrostatic/piezometric pressure. HPT pressure = purple; absolute hydrostatic pressure = med. Blue; corrected HPT pressure = orange; HPT flow = blue dash; Est. K = light blue; slug test K = red box.

measured when an MiHpt log is run includes three basic components: the atmospheric pressure, the hydrostatic pressure (when the probe is below the water table), and the pressure required to inject water into the formation matrix. The HPT QA test run prior to each log gives the ambient atmospheric pressure measured by the transducer. Once the probe is below the water table, advancement is halted and a pressure dissipation test is conducted (Figure 3b). Dissipation tests are usually conducted in low pressure (coarse grained) formations so that pressure dissipation is quick and an accurate measure of the local hydrostatic (piezometric) pressure at that depth is obtained. Given the atmospheric pressure, the hydrostatic pressure at a known depth and the hydrostatic pressure gradient (2.31 ft/psi or 9.81 kPa/m) the Direct Image (DI) Viewer® software will calculate the absolute hydrostatic pressure line and plot it on the pressure log. The absolute hydrostatic pressure and atmospheric pressure may then be subtracted from the total HPT pressure to give the corrected HPT pressure. The corrected HPT pressure is the pressure required to inject water into the formation matrix at the given flow rate. This corrected pressure provides a good measure of relative permeability, with lower pressure indicating higher permeability and vice versa. Equation 1 is used to calculate *Est. K* at each depth interval (Figure 3). After groundwater was sampled at four depth intervals at the SK12 location pneumatic slug tests were run to determine the hydraulic conductivity over each screen interval. Results of the slug tests are plotted

at depth along the *Est. K* log and generally agree with the estimated *K* values (Figure 3).

At the SK04 location the EC value for the three replicate logs is generally low (<50 mS/m) down the entire log with only small variations in response (Figure 4). Apparently, the EC logs here do not give any clear indication of formation lithologic changes with depth as described by Sellwood et al. (2005). However, the corresponding HPT pressure logs display more variability and all three replicate logs show a clear pressure increase below -1.8 m elevation. The SK04 lithologic log indicates a transition to clay till at an elevation of about -2.0 m at this location. It is evident that in this case, the clay till results in an increase in the HPT pressure, but has very little influence on the EC reading.

Again at the SK05 location (Figure 4) EC is generally below 50 mS/m down to an elevation of about -1.5 m. Between about -1.5 and -2.5 m elevation there is a distinct increase in EC to just over 200 mS/m, and then decrease back to around 50 mS/m. The increase in EC begins about 0.5 m before the HPT pressure increases suggesting a possible EC anomaly. Stabilized measurements of specific conductance in water samples collected at multiple depths at the SK05 location reveal an increase in specific conductance as the EC anomaly is approached (Figure 4). Persulfate injections had been conducted upgradient of this location (Figure 2) and sampling in nearby wells showed elevated levels of persulfate and elevated specific conductance (NIRAS 2012). The background log at SK04 together with this information

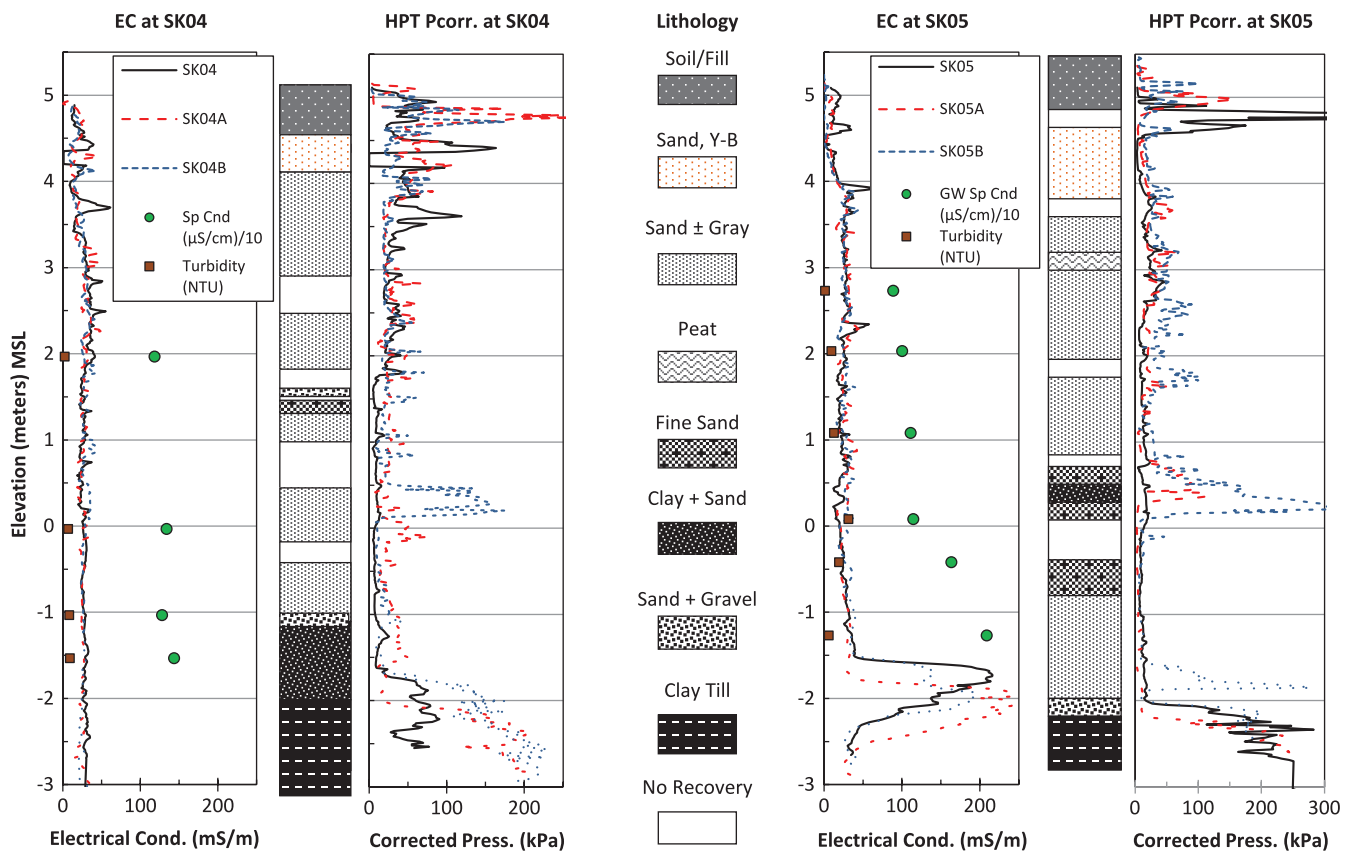


**Figure 4. Comparing lithologic logs based on soil cores to EC and HPT Pressure logs at the SK04 and SK05 locations. Three logs run at both locations about 1.5 m apart to assess variability. MSL = mean sea level; NTU = nephelometric turbidity units;  $\mu\text{S}$  = microSiemen; Sp Cnd = specific conductance of the groundwater; Y-B = yellow to brown, suggesting oxidized; kPa = kiloPascal.**

on persulfate indicates the elevated EC at this and other log locations are the result of persulfate in the aquifer, not increased clay content. The increase in HPT pressure below an elevation of about  $-2.0$  m at SK05 correlates well with the clay till observed in the soil cores. Comparison of the lithologic logs to the HPT pressure logs reveals generally good correlation between the two methods. Because of the low EC of the clay till at this site, and the persulfate anomalies, EC does not provide a good discriminator between the coarse grained and fine grained members of this formation; however, HPT pressure does.

### Contaminant Distributions by MiHpt-XSD, Soil, and Groundwater Sampling

The XSD is sensitive to halogenated compounds and so was used to assess the relative concentration levels and distribution of PCE and its degradation products at the field site (Figure 5).

Relatively low MiHpt-XSD responses ( $<8 \times 10^4 \mu\text{V}$ ) were observed at the SK09 location (Figure 5). Detector peaks were observed primarily in fine grained (higher HPT pressure) zones of the formation while detector baseline (about  $3 \times 10^4 \mu\text{V}$ ) was observed across most of the coarse grained (low HPT pressure) zones in the formation. Soil sample results for total VOCs range from non-detect up to  $116 \mu\text{g}/\text{kg}$  while groundwater samples range between about  $145$  and  $325 \mu\text{g}/\text{L}$  at SK09 (Tables S1 and S2; Figure 5). The bulk of the contaminant observed in the groundwater here was

VC, conversely the soil samples were all non-detect for this compound. The low detector response between elevations of  $2$  and  $-1$  m indicates the MiHpt-XSD detector system did not respond well to the lower levels of the mono- and di-chlorinated X-VOCs in the saturated sandy zones of the formation.

The MiHpt-XSD log at the SK05 location (Figure 5) displays strong detector response ( $>2 \times 10^5 \mu\text{V}$ ) between elevations of  $2$  and  $-1$  m in the formation. This corresponds to the saturated sandy zone of the formation (low HPT pressure). Soil samples collected at this location range from non-detect to just over  $15 \text{ mg}/\text{kg}$  total X-VOCs (Table S1). While higher soil concentrations occur within the zone of elevated XSD response there is a lot of variability in soil sample concentrations. Groundwater was sampled at 6 depth intervals at this location with maximum concentration just over  $70 \text{ mg}/\text{L}$  total X-VOCs (Table S2). The concentration trend of the groundwater sample results closely resembles the zone of contamination defined by the MiHpt-XSD detector log (Figure 5), but is shifted slightly higher in the formation.

MiHpt-XSD detector responses at the SK12 location (Figure 5) are high (up to  $8 \times 10^6 \mu\text{V}$ ) in the fine grained (higher HPT pressure) zone of the formation which is below an elevation of about  $1.8$  m. Again the soil samples exhibit a lot of variability in X-VOC concentration across the zone of elevated detector response (Table S1) but are generally higher where the detector response is elevated. Groundwater samples were collected at six depth intervals at this location.

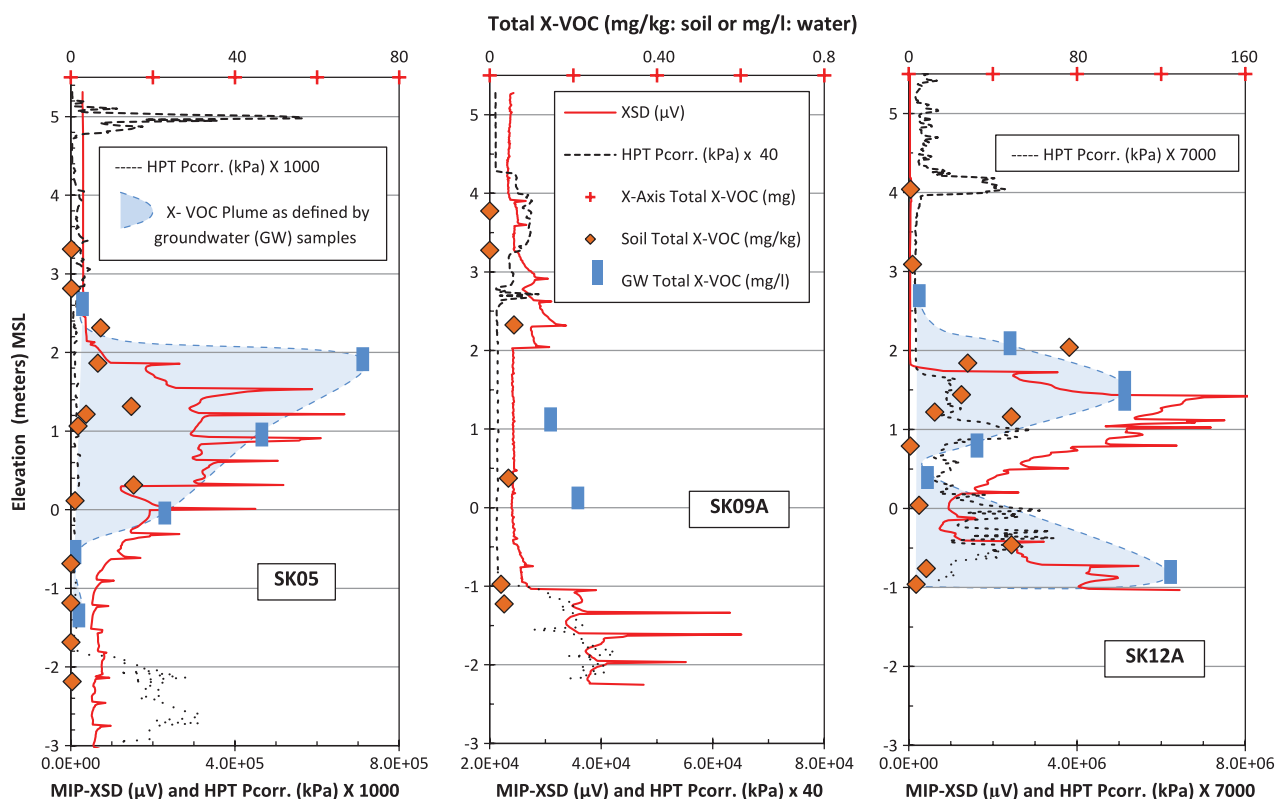


**Figure 5.** Comparison of three logs displaying XSD detector and corrected HPT pressure with soil and groundwater sample results for total X-VOCs. For groundwater sample results vertical length of bar represents screened interval, typically  $30$  cm. The HPT corrected pressure ( $P_{\text{corr}}$ ) is proportionally scaled to plot on the bottom axis. Blue shading indicates contaminant plume as defined by groundwater samples. Note order of magnitude scale differences of horizontal axes between logs for XSD and X-VOC concentrations. MSL = mean sea level; GW = groundwater.

The trend in groundwater total X-VOC concentrations generally mimics the trend defined by the XSD detector response. Again the MiHpt-XSD detector response is slightly shifted to lower elevation relative to the groundwater results.

Overall, the groundwater sample concentrations and distributions correspond well with the XSD detector logs. Increasing sample concentrations corresponding with increasing detector signal and vice versa. There is an apparent downward shift in the MiHpt-XSD system response relative to the groundwater sample results for total X-VOCs at both the SK05 and SK12 locations. An increasing analyte trip time from the membrane to the detector as the log was run, as compared to the trip time measured in the pre-log response test, may cause a downward shift in the XSD log relative to the groundwater sample results. Alternately, development and purging (10+ L) in the short screened piezometers prior to groundwater sampling will decrease the head pressure at the screen. This may have pulled water with higher contamination into the sampler from below the screen interval, resulting in elevated groundwater results for the given interval. Further research will be required to confirm the cause of the small vertical shift observed between the groundwater data and XSD log data.

#### Implications of Field Duplicate and Replicate Sample Results

Groundwater duplicate samples had low relative percent differences (RPDs) (Table S3, Figure S3) and displayed good correspondence with the adjacent MiHpt-XSD

log response (Figure 5), indicating the logs provided a good representation of contaminant level and distribution. Conversely, soil sample results at the same locations and similar depth intervals displayed significant variability and weak correspondence with the groundwater samples and MiHpt-XSD logs (Figure 5; Tables S1 and S2). Eight of seventeen soil duplicate and replicate sample RPDs were greater than 100% (Table S3; Figure S3). Additionally, while all groundwater samples contained VC soil samples from adjacent borings and similar depths were consistently non-detect for this compound (Table S2), demonstrating the loss of VOCs from the soil samples. During field work movement of water through and loss of water from saturated coarse grained samples was observed repeatedly during the soil sampling and subsampling process and may have been responsible for much of the variability seen in the soil analytical results. Because of these factors correlation between soil sample VOC results and MiHpt detector logs were poor at this site. Furthermore, similar conditions at other sites may impact the correlation of soil sample results with MiHpt detector logs. (Additional information regarding duplicate and replicate sampling and results is provided in the Supporting Information.)

#### Integrating Log Data for Interpretation

Reviewing logs with all of the primary data enables the investigator to easily observe the subsurface conditions (Figure 6). Low EC and low HPT pressure observed down to an elevation of about -2 m at SK05 indicates that the

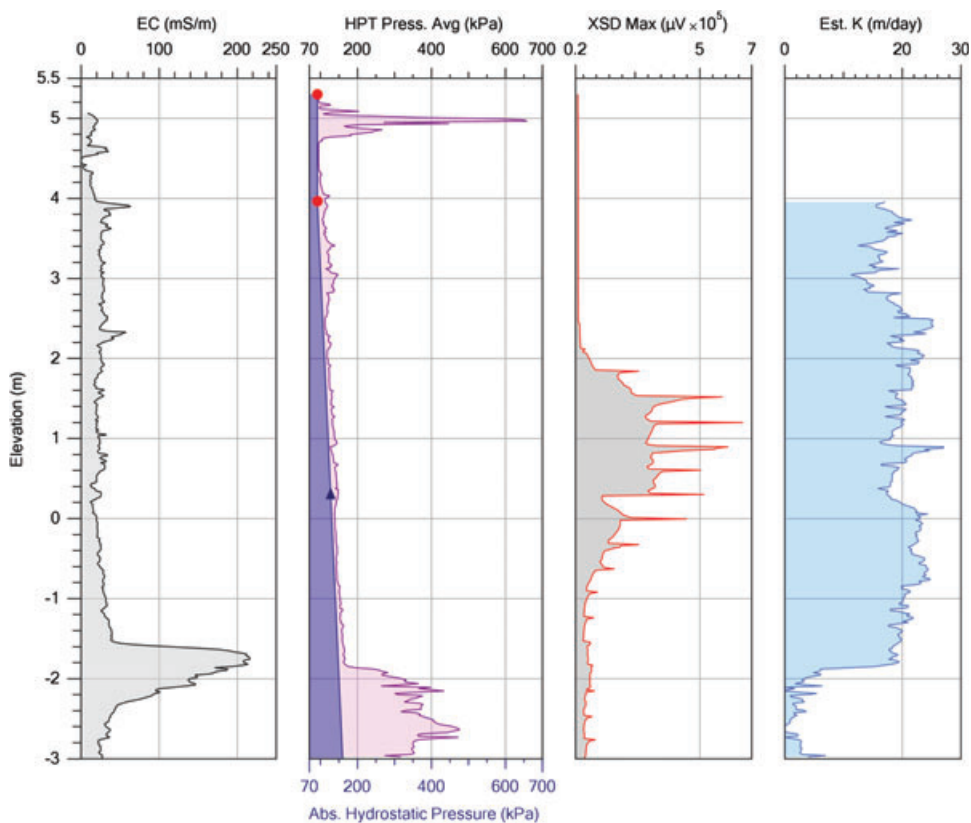


**Figure 6.** MiHpt log from the SK05 location displaying primary log parameters. Left to right: EC, HPT pressure with hydrostatic profile, XSD, and estimated hydraulic conductivity (Est. K). Elevation reference is mean seal level.



formation is primarily coarse grained with a static water level at about 4 m elevation. Below about -2 m elevation, increased HPT pressure indicates that a fine grained/lower permeability material is encountered (clay till). The increase in EC starting above the increase in HPT pressure suggests the presence of an ionic contaminant (in this case injected persulfate remediation fluid). The XSD detector defines a zone of X-VOC contamination between about 2.5 to 1.0 m of elevation. Looking at the HPT pressure and *Est. K* log reveals that the majority of the contaminant mass is located in the permeable coarse grained zone of the formation where hydraulic conductivity is near 20 m/d. Therefore, at this location the contaminant mass is located in a very effective migration pathway.

### Example of Site Interpretation Using an MiHpt Log Cross Section

A simple two-dimensional cross section of the logs at the Skuldelev field site (Figure 7) is based on the HPT pressure and MiHpt-XSD detector responses (shaded). Comparison of core samples to HPT pressure logs demonstrated that increased pressure at depth correlates with the clay till underlying the site. Looking at the HPT pressure logs across the section it is apparent that the depth to the top of the clay till (higher pressure) varies from an elevation of about 1 m at the SK01 log to about -2 m at the SK05 log. A green dotted line is drawn on the cross section along the

top of the clay till (increased pressure) in each log. On the basis of core sample information and the HPT pressure logs it is apparent that this line corresponds to a paleo-erosion surface in the underlying clay till probably cut by a late glacial stream. This old erosion surface appears to form a small paleo-valley which is now filled with sand and gravel (low HPT pressure) deposited later, possibly glacial outwash.

Looking at the MiHpt-XSD log responses on the cross section (Figure 7) it is apparent that there are two separate hot spots of X-VOC contamination delineated by the logs. One of the hot spots occurs around logs SK05 and SK07 near the center of the transect. Here the X-VOC contamination is present primarily in the low HPT pressure, coarse grained materials (sands and gravels). Along the west end of the transect at logs SK11 and SK12 the contamination appears to be present primarily in the fine grained clay till material and almost absent in the overlying sands and gravels. The origin of these two X-VOC hot spots is quite different and helps to explain why the contaminants are associated with very different lithology. A review of site information (NIRAS 2010) found that the hot spot at SK05 and SK07 is a transect across the groundwater plume flowing from the source area and migrating down gradient via groundwater flow (Figure 2). Conversely, the hot spot at the west end of the transect at SK12 originated from a sewer leak after solvents were disposed of in the wastewater sewer at the facility. Also note, the groundwater VOC plume appears to

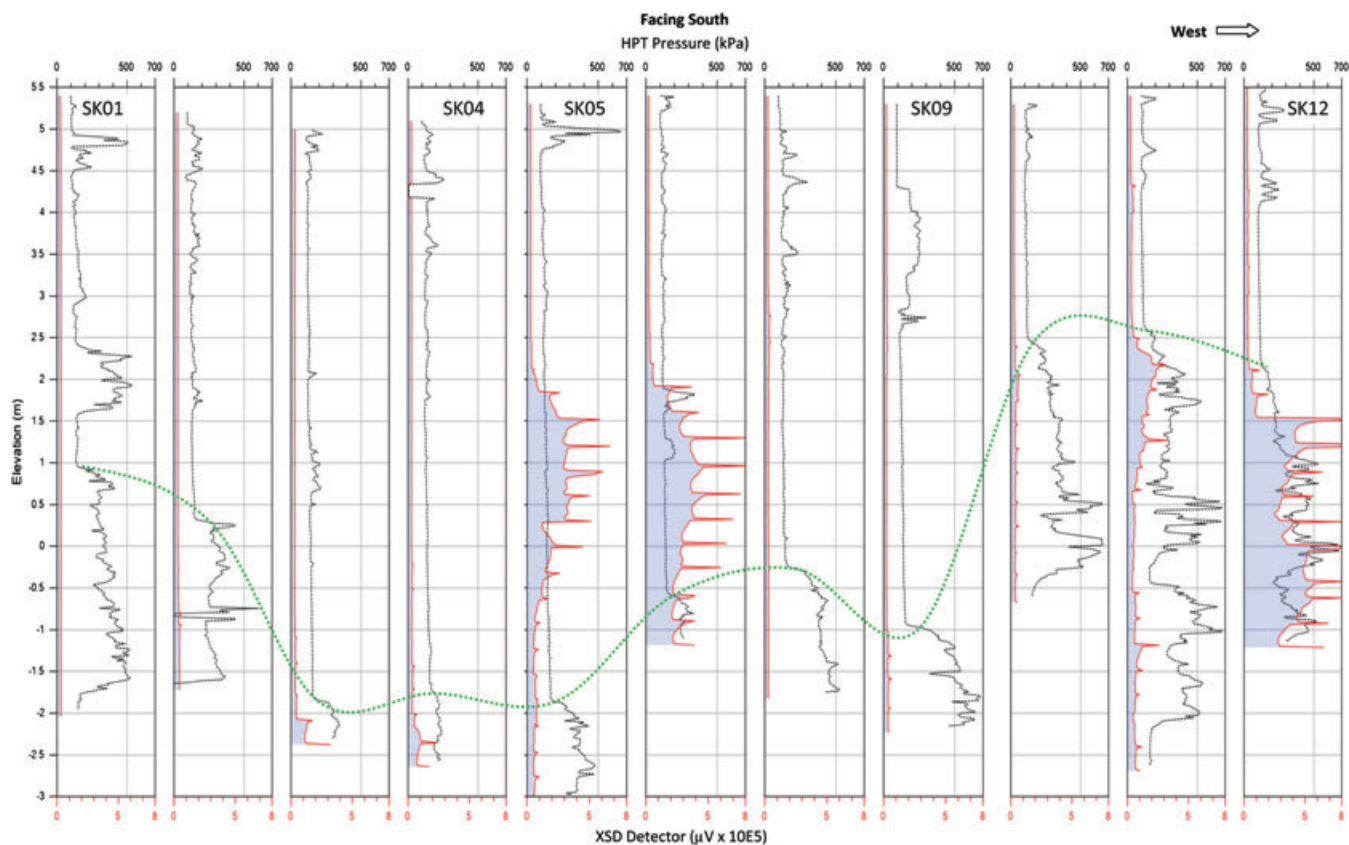


Figure 7. Simple two-dimensional cross section at the Skuldelev site, elevation reference is mean sea level. MiHpt logs were run in a general E-W line across the site (see Figure 2 for log and transect locations). HPT pressure (black dashed lines), XSD detector response (red lines with blue fill), the green dashed line traces the top of the clay till based on HPT pressure. Spacing between logs is approximately 8 m.



be migrating along the buried stream valley defined by the HPT pressure logs.

## Summary and Conclusions

The MiHpt-XSD detector system was effective at determining the general distribution and relative concentrations of the X-VOC contaminants at Skuldelev. The contaminant distribution as defined by the groundwater samples was very similar to the plume as defined by the MiHpt-XSD detector logs. However, the groundwater plume was shifted slightly higher in the formation relative to the plume defined by the MiHpt-XSD detector logs. This may be the result of a delay in response to the MiHpt-XSD detector system, possibly resulting from a low trip-time value or decreasing flow rate for the carrier gas as the log was run. Further investigation will be required to confirm the cause of the small detector log shift and define a corrective measure.

While groundwater samples corresponded well to MiHpt-XSD detector results, soil sample results were found to vary significantly at the same location and similar depth intervals. Field observations (drainage of pore water) and assessment of duplicate and replicate samples indicate that soil sampling for VOCs often suffers from several inherent limitations (heterogeneity, loss of VOCs, etc.) and analytical results may not be reliable for comparison to MiHpt-XSD logs under some field conditions.

Groundwater samples collected adjacent to a non-detect MiHpt-XSD log were found to contain VC and DCE in the 100 to 300 µg/L concentration range. This indicates that the current MiHpt-XSD system has difficulty detecting these analytes in this concentration range in the saturated coarse grained formation investigated. Development of a low-level MIP system is underway at this time and should lower detection levels for the MIP system by a factor of 3× to 10× depending on the specific contaminant and formation conditions.

At Skuldelev the clay till unexpectedly exhibited low EC similar to that observed in the adjacent sands and gravels. Due to this the EC logs could not clearly distinguish between the coarse and fine grained facies of the local formation. The HPT pressure logs clearly defined the difference in permeability between the clay till (high HPT pressure) and coarse-grained sediments (low HPT pressure). The HPT pressure response was confirmed with soil coring at selected locations and discrete interval slug testing at one location.

A simple two-dimensional cross section was constructed with the MiHpt-XSD detector logs and pressure logs. The cross section was useful in understanding contaminant distribution and the influence of the local hydrostratigraphy on contaminant migration. Several years of previous investigation at the site had not determined what was controlling the migration path of the groundwater plume. The transect of MiHpt pressure logs revealed a buried stream valley cut in the clay till underlying the site, along which the groundwater X-VOC plume is migrating.

Overall, the MiHpt detector logs proved useful in defining contaminant distribution and levels while the HPT pressure logs defined lithologic changes and hydrostratigraphic architecture that are important in understanding contaminant

migration. The study results indicate that the high-resolution data from the MiHpt logs provide a powerful tool for defining an accurate site conceptual model and should prove valuable when developing a remediation strategy.

## Acknowledgments

This study was supported in part by funding from the Department of Environment of the Capital Region of Denmark. We would like to express our appreciation to the NIRAS field team, especially Robert Berlowicz and Peter Thompsen, all of whom worked long hours to complete this research. The coauthors would also like to express their appreciation to Mads Terkelsen at the Capital Region of Denmark for his efforts and support that made this work possible. We would also like to thank the technical reviewers and editors for comments that substantially improved the manuscript.

## Supporting Information

The following supporting information is available for this article:

**Table S1.** Soil analytical data for X-VOCs.

**Table S2.** Groundwater analytical data for X-VOCs.

**Table S3.** Field duplicate and replicate sample results with RPDs.

**Figure S1.** Components of the MiHpt system.

**Figure S2.** Field methods and procedures.

**Figure S3.** Evaluation of duplicate and replicate samples.

## References

- American Society for Testing and Materials (ASTM). 2007a. Standard practice for direct push technology for volatile contaminant logging with the membrane interface probe (MIP). In *Annual Book of ASTM Standards, Vol. 04.09 Soil and Rock (II)*. West Conshohocken, Pennsylvania: ASTM International. www.astm.org.
- ASTM. 2007b. D6282 standard guide for direct push soil sampling for environmental site characterization. In *Annual Book of ASTM Standards, Vol. 04.09 Soil and Rock (II)*. West Conshohocken, Pennsylvania: ASTM International. www.astm.org.
- ASTM. 2007c. D6001 standard guide for direct-push ground water sampling for environmental site characterization. In *Annual Book of ASTM Standards, Vol. 04.09 Soil and Rock (II)*. West Conshohocken, Pennsylvania: ASTM International. www.astm.org.
- ASTM. 2007d. D6771 standard practice for wells and devices used for ground-water quality investigations. In *Annual Book of ASTM Standards, Vol. 04.09 Soil and Rock (II)*. West Conshohocken, Pennsylvania: ASTM International. www.astm.org.
- Bohling, G.C., G. Liu, S.J. Knobbe, E.C. Reboulet, D.W. Hyndman, P. Dietrich, and J.J. Butler Jr. 2012. Geostatistical analysis of centimeter-scale hydraulic conductivity variations at the MADE site. *Water Resources Research* 48: 15. W02525. DOI: 10.1029/2011WR010791.
- Bowling, J.C., A.B. Rodriguez, D.L. Harry, and C. Zheng. 2005. Delineating alluvial aquifer heterogeneity using resistivity and GPR data. *Ground Water* 43, no. 6.
- Bright, J., F. Wang, and M. Close. 2002. Influence of the amount of available K data on uncertainty about contaminant transport prediction. *Ground Water* 40, no. 5: 529–534.

- Bronders, J., I. Van Keer, K. Touchant, G. Vanermen, and D. Wilczek. 2009. *Journal Soils Sediments* 9: 74–82. DOI: 10.1007/s11368-008-0054-9.
- Bumberger, J., D. Radny, A. Berndsen, T. Goblirsch, J. Flachowsky, and P. Dietrich. 2011. Carry-over effects of the membrane interface probe. *Ground Water* 50, no. 4, 578–584.
- Christy, T.M., 1996. A driveable permeable membrane sensor of volatile compounds in soil. In *Proceedings for the detection of the Tenth National Outdoor Action Conference*, 169–177. Dublin, Ohio: National Ground Water Association.
- Christy, C.D., T.M. Christy, and V. Wittig. 1994. A percussion probing tool for the direct sensing of soil conductivity. In *Proceedings of the 8th National Outdoor Action Conference*, 381–394. Dublin, Ohio: National Ground Water Association. www.ngwa.org.
- Christy, T.M., and S.C. Spradlin, 1992. The use of small diameter probing equipment for contaminated site investigation. In *Proceedings of the Sixth National Outdoor Action Conference*, 87–101. Dublin, Ohio: National Ground Water Association.
- Considine, T., and A. Robbat, Jr. 2008. On-site profiling and speciation of polycyclic aromatic hydrocarbons at manufactured gas plant sites by a high temperature transfer line, membrane inlet probe coupled to a photoionization detector and gas chromatograph/mass spectrometer. *Environmental Science and Technology* 2, no. 4, 1213–1220.
- Costanza, J., and W.M. Davis. 2000. Rapid detection of volatile organic compounds in the subsurface by membrane introduction into a direct sampling ion-trap mass spectrometer. *Field Analytical Chemistry and Technology* 4, no. 5: 246–254.
- Devlin, J.F., P.C. Schilling, I. Bowen, C.E. Critchley, D.L. Rudolph, N.R. Thomson, G.P. Tsoflias, J.A., Roberts. 2012. Applications and implications of direct groundwater velocity measurement at the centimeter scale. *Journal of Contaminant Hydrology* 127: 3–14.
- Environmental Protection Agency (EPA). 2013. High-resolution site characterization (HRSC). <http://www.clu-in.org/characterization/technologies/hrsc> (accessed August 14, 2013).
- Environmental Protection Agency (EPA). 2011. Environmental cleanup best management practices: Effective use of the project life cycle conceptual site model. OSWER (5102G). EPA 542-F-11-011. Washington, DC: U.S. Environmental Protection Agency. <http://www.epa.gov/tio/download/remed/csm-life-cycle-fact-sheet-final.pdf> (accessed August 14, 2013).
- Environmental Protection Agency (EPA). 2010. Best management practices: Use of systematic project planning under a triad approach for site assessment and cleanup. OSWER (5203P). EPA 542-F-10-010. Washington, DC: U.S. Environmental Protection Agency. [http://www.brownfieldstsc.org/pdfs/SPPBulletin\\_forWeb.pdf](http://www.brownfieldstsc.org/pdfs/SPPBulletin_forWeb.pdf) (accessed August 14, 2013).
- Environmental Protection Agency (EPA). 1998. Seminars: Monitored natural attenuation for ground water. EPA/625/K-98/001. Washington, DC: U.S. Environmental Protection Agency Office of Research and Development.
- Geoprobe. 2011a. Geoprobe® DT325 Dual Tube Sampling System, Standard Operating Procedure. Technical Bulletin No. MK3138. Salina, Kansas: Kejr Inc. www.geoprobe.com.
- Geoprobe. 2011b. Geoprobe® Model MB470 Mechanical Bladder Pump, Standard Operating Procedure. Technical Bulletin No. MK3013. Salina, Kansas: Kejr Inc. www.geoprobe.com.
- Geoprobe. 2009. Geoprobe® Membrane Interface Probe (MIP) Standard Operating Procedure. Technical Bulletin No. MK3010. Salina, Kansas: Kejr Inc. Prepared 2003. Revised 2009. www.geoprobe.com.
- Geoprobe. 2007. Geoprobe® Hydraulic Profiling Tool (HPT) System Standard Operating Procedure. Technical Bulletin No. MK3137. Salina, Kansas: Kejr, Inc. www.geoprobe.com.
- Geoprobe. 2006a. Hydrostratigraphic characterization using the hydraulic profiling tool (HPT). Technical Bulletin MK3099. Salina, Kansas: Kejr, Inc. www.geoprobe.com.
- Geoprobe. 2006b. Geoprobe® Screen Point 16 Groundwater Sampler, Standard Operating Procedure. Technical Bulletin No. MK3142. Salina, Kansas: Kejr, Inc. www.geoprobe.com.
- Geoprobe. 2004. Geoprobe® Direct Image® MP6500 Membrane Interface Probe (MIP) Controller User Manual. Document No. MK3083, Revision 1.00. Salina, Kansas: Kejr Inc. www.geoprobe.com.
- Griffin, T.W., and K.W. Watson. 2002. A comparison of techniques for confirming dense nonaqueous phase liquids. *Ground Water Monitoring & Remediation* 20, no. 2: 48–59.
- Interstate Technology & Regulatory Council (ITRC). 2011. Integrated DNAPL Site Strategy. IDSS-1. ITRC Integrated DNAPL Site Strategy Team. www.itrcweb.org.
- ITRC. 2010. Use and measurement of mass flux and mass discharge. MASSFLUX-1. Washington, DC: ITRC Integrated DNAPL Site Strategy Team. www.itrcweb.org.
- Kober, R., G. Hornbruch, C. Leven, L. Tischer, J. Großmann, P. Dietrich, H. Weiß, and A. Dahmke. 2009. Evaluation of combined direct-push methods used for aquifer model generation. *Ground Water* 47, no. 1: 536–546.
- Kurup, P.U. 2009. Novel technologies for sniffing soil and ground water contaminants. *Current Science* 97, no. 8: 1212–1219.
- Lunne, T., P.K. Robertson, J.J.M. Powell. 1997. *Cone Penetration Testing in Geotechnical Practice*, 312. London, UK and New York: Spon Press/Taylor and Francis Group.
- McAndrews, B., K. Heinze, and W. DiGuseppi. 2003. Defining TCE plume source areas using the membrane interface probe (MIP). *Soil and Sediment Contamination: An International Journal* 12, no. 6: 799–813. DOI: 10.1080/714037716.
- McCall, W. 2012. Draft final report: Field demonstration of the combined membrane-interface probe and hydraulic profiling tool (MiHpt), 63.
- McCall, W. 2011. Application of the Geoprobe® HPT logging system for geo-environmental investigations. Geoprobe® Technical Bulletin No. MK3184. Salina, Kansas: Kejr, Inc. www.geoprobe.com.
- McCall, W. 2010. Tech guide for calculation of estimated hydraulic conductivity (Est. K) log from HPT data. Salina, Kansas: Kejr Inc. www.geoprobe.com.
- McCall, W. 2005. Evaluation of a small mechanical and pneumatic bladder pump for water quality sampling. *Ground Water Monitoring & Remediation* 25, no. 2, 145–153.
- McCall, W., and T.M. Christy. 2010. Abstract: Development of a hydraulic conductivity estimate for the hydraulic profiling tool. Paper Presented at the 2010 North American Environmental Field Conference & Exposition. Conference Program with Abstracts. Las Cruces, New Mexico: The Nielsen Environmental Field School.
- McCall, W., D.M. Nielsen, S.P. Farrington, and T.M. Christy. 2006. Use of direct push technologies in environmental site characterization and ground-water monitoring, *Practical Handbook of Environmental Site Characterization and Ground-Water Monitoring*, Chapter 6, 2nd ed. Boca Raton, Florida: CRC Press/Taylor & Francis Group.
- NIRAS A/S. 2012. Trip report: Test of combined membrane interface probe and hydraulic profiling tool. Allerød, Denmark: Skuldelev, DK. NIRAS A/S. www.niras.com.
- NIRAS A/S. 2010. Skuldelev: Afgrænsende Undersøgelser Ved Hot-Spot Område IV. Allerød, Denmark: NIRAS A/S. www.niras.com.
- Payne, F.C., J.A. Quinnan, and S.T. Potter. 2008. Remediation hydraulics, 408. Boca Raton, Florida: CRC Press.

- Ravella, M., R.J. Fiacco, Jr., J. Frazier, D. Wanty, and L. Burkhardt. 2007. Application of the membrane interface probe (MIP) to delineate subsurface DNAPL contamination. *Environmental Engineer: Applied Research and Practice* 1. <http://www.aaee.net>
- Sanchez-Vila, X., J. Carrera, and J.P. Girardi. 1996. Scale effects in Transmissivity. *Journal of Hydrology* 183: 1–22.
- Schulmeister, M.K., J.J. Butler, Jr., E.K. Franseen. 2004. High-resolution stratigraphic characterization of unconsolidated deposits using direct-push electrical conductivity logging: A floodplain-margin example. In *Aquifer Characterization*. Society for Sedimentary Geology, Tulsa, OK. Special Publication no. 80, 67–78.
- Schulmeister, M.K., J.J. Butler Jr., J.M. Healey, L. Zheng, D.A. Wysocki, and G.W. McCall. 2003. Direct-push electrical conductivity logging for high-resolution hydrostratigraphic characterization. *Ground Water Monitoring & Remediation* 23, no. 3: 52–62.
- Sellwood, S.M., J.M. Healey, S. Birk, and J.J. Butler, Jr. 2005. Direct-push hydrostratigraphic profiling: Coupling electrical logging and slug tests. *Ground Water* 43, no. 1: 19–29.
- Wilson, J.T., R.R. Ross, and S. Acree. 2005. Using direct-push tools to map hydrostratigraphy and predict MTBE plume diving. *Ground Water Monitoring & Remediation* 25, no. 3: 93–102. [www.ngwa.org](http://www.ngwa.org).
- Wilson, J.T., J.S. Cho, F.P. Beck, and J.A. Vardy. 1997. Field estimation of hydraulic conductivity for assessments of natural attenuation. *Bioremediation* 4, no. 2: 309–314.
- Zheng, C., and S.M. Gorelick. 2003. Analysis of solute transport flow fields influenced by preferential flowpaths at the decimeter scale. *Groundwater* 41, no. 2: 142–155.

## Biographical Sketches

**Wesley McCall**, PG, corresponding author, Geologist (KS28), Geoprobe Systems, Inc., 1835 Wall St, Salina, KS 67401; 785-825-1842; fax 785-825-6983; [mccallw@geoprobe.com](mailto:mccallw@geoprobe.com)

**Thomas M. Christy**, PE, Vice President, Geoprobe Systems, Inc., 1835 Wall St., Salina, KS 67401; 785-825-1842; fax 785-825-6983; [christyt@geoprobe.com](mailto:christyt@geoprobe.com)

**Daniel A. Pipp**, Chemist, MIP Specialist, Geoprobe Systems, Inc., 1835 Wall St, Salina, KS 67401; 785-825-1842; fax 785-825-6983; [pippd@geoprobe.com](mailto:pippd@geoprobe.com)

**Mads Terkelsen**, M.Sc., Research and Development Manager, Department of Environment, Capital Region, Denmark. Kongens Vaenge 2, 3400 Hilleroed, Denmark; +45-38665615; [mte@regionh.dk](mailto:mte@regionh.dk)

**Anders G. Christensen**, M.Sc., NIRAS A/S, Sortemosevej 19, DK-3450 Alleroed, Denmark; +45-48104405; fax +45-48104300; [agc@niras.dk](mailto:agc@niras.dk)

**Klaus Weber**, M.Sc., NIRAS A/S, Sortemosevej 19, DK-3450 Alleroed, Denmark; +45-48104233; fax +45-48104300; [kwe@niras.dk](mailto:kwe@niras.dk)

**Peter Engelsen**, M.Sc., NIRAS A/S, Sortemosevej 19, DK-3450 Alleroed, Denmark; +45-48104200; fax +45-48104300; [pen@niras.dk](mailto:pen@niras.dk)